

Silicon-Naphthalo/Phthalocyanine-Hybrid Sensitizer for Efficient Red Response in Dye-Sensitized Solar Cells

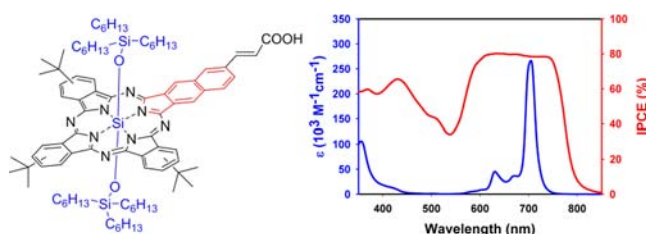
Bogyu Lim,^{†,⊥} George Y. Margulis,^{‡,⊥} Jun-Ho Yum,[§] Eva L. Unger,[†] Brian E. Hardin,^{||} Michael Grätzel,[§] Michael D. McGehee,[†] and Alan Sellinger^{*,†,§}

Department of Materials Science and Engineering, Stanford University, Stanford, California 94305, United States, Department of Applied Physics, Stanford University, Stanford, California 94305, United States, Molecular Foundry, Lawrence Berkeley National Laboratory, Berkeley, California 94720, United States, and Laboratory for Photonics and Interfaces, Institute of Chemical Sciences and Engineering, School of Basic Science, Ecole Polytechnique Fédérale de Lausanne, CH-1015 Lausanne, Switzerland

aselli@mines.edu

Received December 16, 2012

ABSTRACT



Introduction of a naphthalocyanine moiety to phthalocyanine allows for a gradual red shift of the absorption spectrum in the resulting chromophore. Using silicon as a core atom allows for the introduction of additional siloxane side chains which mitigate dye aggregation. A dye-sensitized solar cell with this hybrid sensitizer exhibits a broad and flat IPCE of 80% between 600 and 750 nm and high photocurrent densities of 19.0 mA/cm².

Dye-sensitized solar cells (DSCs) have attracted considerable attention because of their low manufacturing cost and use of nontoxic materials.¹ DSCs using polypyridyl-ruthenium complexes as sensitizers have achieved power conversion efficiencies (PCE) of 11.5% under AM 1.5

irradiation.² However, the weak absorption coefficient of these sensitizers in the red and scarcity of ruthenium have pushed the development of efficient red-sensitive and ruthenium-free sensitizers for DSCs. Low band gap sensitizers with extended π -conjugation such as porphyrins and phthalocyanines have shown particular promise due to efficient photoinduced electron-transfer and high absorption coefficients in the red region of the solar spectrum.³ Recently, Grätzel et al. reported a new record DSC-efficiency of over 12% using a zinc-porphyrin dye in combination with a cobalt redox shuttle.⁴ Additionally, strongly absorbing low band gap sensitizers can be used in conjunction with strategies such as energy relay dyes or

[†] Department of Materials Science and Engineering, Stanford University.

[‡] Department of Applied Physics, Stanford University.

[§] Ecole Polytechnique Fédérale de Lausanne.

^{||} Lawrence Berkeley National Laboratory.

[⊥] These authors contributed equally.

^{*} Current address: Department of Chemistry and Geochemistry, Colorado School of Mines, Golden, CO 80401, USA.

(1) (a) Grätzel, M. *Nature* **2001**, *414*, 338. (b) O'Regan, O.; Grätzel, M. *Nature* **1991**, *353*, 737. (c) Hardin, B. E.; Snaith, H. J.; McGehee, M. D. *Nat. Photonics* **2012**, *6*, 162. (d) Hagfeldt, A.; Boschloo, G.; Sun, L.; Kloo, L.; Pettersson, H. *Chem. Rev.* **2010**, *110*, 6595.

(2) (a) Nazeeruddin, M. K.; De Angelis, F.; Fantacci, S.; Selloni, A.; Viscardi, G.; Liska, P.; Ito, S.; Takeru, B.; Grätzel, M. *J. Am. Chem. Soc.* **2005**, *127*, 16835. (b) Chen, C.-Y.; Wang, M.; Li, J.-Y.; Pootrakulchote, N.; Alibabaei, L.; Ngoc-le, C.-H.; Decoppet, J.-D.; Tsai, J.-H.; Grätzel, M.; Wu, C.-G.; Zakeeruddin, S. M.; Grätzel, M. *ACS Nano* **2009**, *3*, 3103. (c) Han, L.; Islam, A.; Chen, H.; Malapaka, C.; Chiranjeevi, B.; Zhang, S.; Yang, X.; Yanagida, M. *Energy Environ. Sci.* **2012**, *5*, 6057.

(3) (a) Bessho, T.; Zakeeruddin, S. M.; Yeh, C.-Y.; Diau, E. W.-G.; Grätzel, M. *Angew. Chem., Int. Ed.* **2010**, *49*, 6646. (b) Yum, J.-H.; Jang, S.-R.; Humphry-Baker, R.; Grätzel, M.; Cid, J.-J.; Torres, T.; Nazeeruddin, M. K. *Langmuir* **2008**, *24*, 5636.

(4) Yella, A.; Lee, H.-W.; Tsao, H. N.; Yi, C.; Chandiran, A. K.; Nazeeruddin, M. K.; Diau, E. W.-G.; Yeh, C.-Y.; Zakeeruddin, S. M.; Grätzel, M. *Science* **2011**, *334*, 629.

cosensitization to achieve an efficient panchromatic photo-response.⁵ It should also be noted that such efficient low band gap sensitizers are necessary for applications in DSC tandems, which may be necessary to achieve the efficiencies required for widespread DSC commercialization.⁶

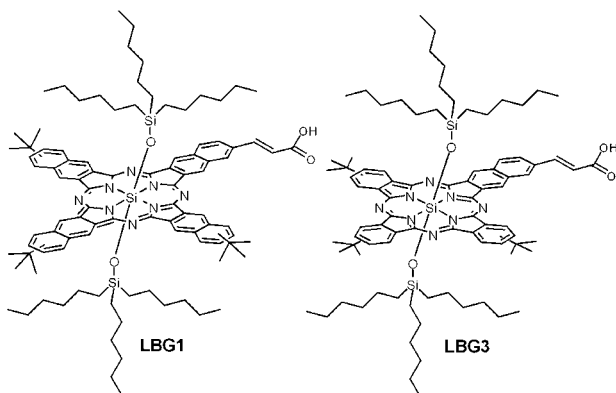


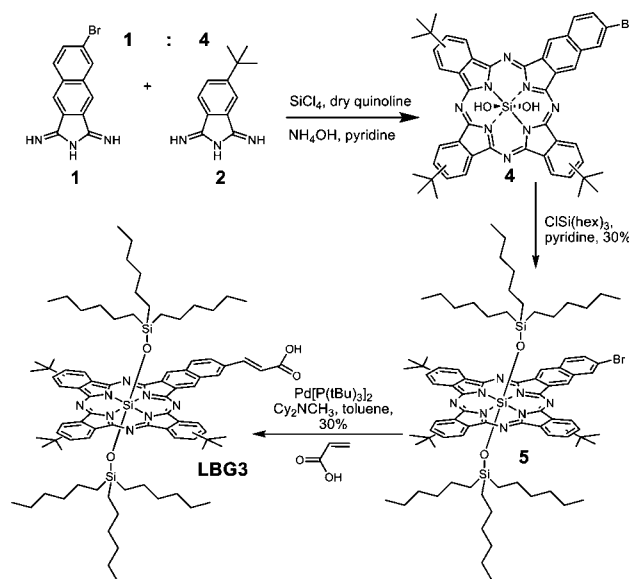
Figure 1. Molecular structures of **LBG1** and **LBG3** dyes.

To further increase the efficiency of DSCs, sensitizers that harvest photons in the red and near-infrared region need to be developed.^{1c} This is a difficult task as the energy levels of low band gap dyes are constrained by the thermodynamic requirements of DSCs. Dyes must have sufficient driving force for photoinduced charge carrier injection into titania and regeneration by the redox mediator, and consequently, very few dyes have shown high light harvesting efficiency beyond 750 nm.

Among red-sensitive dyes investigated in DSCs, phthalocyanines (Pcs) have exhibited high performance with light harvesting efficiency up to 700 nm as well as good thermal and photochemical stability.⁷ While zinc-phthalocyanine (ZnPc)-based dyes exhibit a strong tendency to form H-aggregates on the TiO₂ surface due to cofacial π - π interactions between the macrocycle discs,^{7,8} this can be reduced by the presence of bulky substituents, such as 2,6-diphenylphenoxy groups.⁹ However, the absorption spectrum of Pc-based dyes drops off sharply

below 700 nm, not allowing for strong light harvesting in the far red and infrared. Naphthalocyanines (Ncs) are interesting due to their more red-shifted absorption with respect to Pcs.¹⁰ To date, Ncs employed as sensitizers for DSCs have exhibited a device efficiency of only 0.1%, presumably due to poor charge injection efficiency.¹¹

Scheme 1. Synthesis of **LBG3**



Herein, we report and characterize two novel silicon-naphthalo/phthalocyanine-based sensitizers, coded **LBG1** and **LBG3** (Figure 1). **LBG1** is a silicon-naphthalocyanine dye based on a previously investigated Zn-naphthalocyanine which exhibited poor solubility.¹² The second dye, **LBG3**, has a mononaphthalo-triphthalocyanine core,⁸ which can thus be considered a hybrid between a Pc and Nc dye. In solar cell devices, it was found that **LBG1** exhibited low photovoltaic performance that could be rationalized by a lack of thermodynamic driving force for both the photoinduced injection of electrons into TiO₂ and the regeneration of the dye by the iodide/triiodide based redox electrolyte. The mixed dye **LBG3**, however, exhibited high photocurrents and an excellent photo-response at wavelengths beyond 750 nm, a rarity for efficient DSC sensitizers. This hybrid SiNcPc approach is shown to not only tune energy levels but also maintain solubility and high extinction coefficients.

For both dyes, bulky *tert*-butyl substituents were added to the core periphery, and trihexylsiloxy groups were introduced as coordinating ligands to the silicon center. The introduction of *tert*-butyl and trihexylsiloxy groups

(5) (a) Hardin, B. E.; Hoke, E. T.; Armstrong, P. B.; Yum, J.-H.; Comte, P.; Torres, T.; Fréchet, J. M. J.; Nazeeruddin, M. K.; Grätzel, M.; McGehee, M. D. *Nat. Photonics* **2009**, *3*, 406. (b) Yum, J.-H.; Hardin, B. E.; Moon, S.-J.; Baranoff, E.; Nüesch, F.; McGehee, M. D.; Grätzel, M.; Nazeeruddin, M. K. *Angew. Chem., Int. Ed.* **2009**, *48*, 9277. (c) Hardin, B. E.; Yum, J.-H.; Hoke, E. T.; Jun, Y. C.; Péchy, P.; Torres, T.; Brongersma, M. L.; Nazeeruddin, M. K.; Grätzel, M.; McGehee, M. D. *Nano Lett.* **2010**, *10*, 3077. (d) Shrestha, M.; Si, L.; Chang, C.-W.; He, H.; Sykes, A.; Lin, C.-Y.; Diau, E. W.-G. *J. Phys. Chem. C* **2012**, *116*, 10451.

(6) Nattestad, A.; Mozer, A. J.; Fischer, M. K. R.; Cheng, Y.-B.; Mishra, A.; Bäuerle, P.; Bach, U. *Nat. Mater.* **2010**, *9*, 31.

(7) López-Duarte, I.; Wang, M.; Humphry-Baker, R.; Ince, M.; Martínez-Díaz, M. V.; Nazeeruddin, M. K.; Torres, T.; Grätzel, M. *Angew. Chem., Int. Ed.* **2012**, *51*, 1895.

(8) Yu, L.; Zhou, X.; Yin, Y.; Liu, Y.; Li, R.; Peng, T. *Chem-PlusChem* **2012**, *77*, 1022.

(9) (a) Mori, S.; Nagata, M.; Nakahata, Y.; Yasuta, K.; Goto, R.; Kimura, M.; Taya, M. *J. Am. Chem. Soc.* **2010**, *132*, 4054. (b) Ragoussi, M.-E.; Cid, J.-J.; Yum, J.-H.; Torre, G.; de la; Di Censo, D.; Grätzel, M.; Nazeeruddin, M. K.; Torres, T. *Angew. Chem., Int. Ed.* **2012**, *51*, 4375.

(10) Kobayashi, N.; Nakajima, S.; Ogata, H.; Fukuda, T. *Chem.—Eur. J.* **2004**, *10*, 6294–312.

(11) Macor, L.; Fungo, F.; Tempesti, T.; Durantini, E. N.; Otero, L.; Barea, E. M.; Fabregat-Santiago, F.; Bisquert, J. *Energy Environ. Sci.* **2009**, *2*, 529.

(12) Hardin, B. E.; Sellinger, A.; Moehl, T.; Humphry-Baker, R.; Moser, J.-E.; Wang, P.; Zakeeruddin, S. M.; Grätzel, M.; McGehee, M. D. *J. Am. Chem. Soc.* **2011**, *133*, 10662.

reduces molecular aggregation as well as increases solubility. The lateral bulky siloxy groups were specifically introduced to prevent the formation of H-aggregates, but it was found that their presence leads to a tendency for the formation of J-aggregates (see Figure S16).¹³ Furthermore, bulky substituents could reduce interfacial recombination.⁷ In addition, vinyl linking groups were used to establish a conjugated connection between the carboxylic acid anchoring unit and the core dye molecule.^{9b}

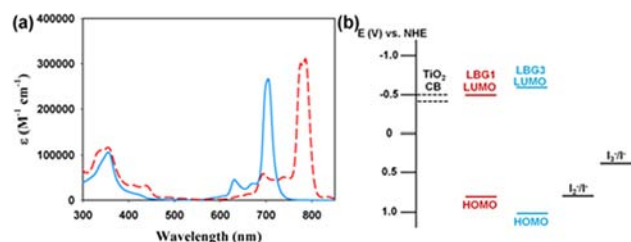


Figure 2. (a) Absorption spectra in CHCl_3 ($c = 10^{-5} \text{ M}$), and (b) a schematic energy-level diagram of **LBG1** (red) and **LBG3** (blue).

The synthesis of both dyes is described in the Supporting Information. An example synthetic procedure for **LBG3** is shown in Scheme 1. In the case of **LBG3**, the hydroxyl compound (**4**) was synthesized in two steps from a 4:1 ratio of 5-*tert*-butyl-1,3-diiminoisindoline (**2**) to 6-bromo-1,3-diiminobenz[*f*]isindoline (**1**). Due to the insolubility of the hydroxyl compound (**4**) in organic solvents, it was used for subsequent reactions without further purification. The silylation of **4** resulted in compound **5** and *tert*-butyl silicon-phthalocyanine (*tert*-butyl SiPc, Figure S1) as a byproduct. Because both **5** and the *tert*-butyl SiPc byproduct have the same polarity, *tert*-butyl SiPc was separated following the Heck-coupling reaction with acrylic acid. One of the key steps in this procedure is the introduction of the carboxylic acid group in the final step using mild Heck reaction conditions. It was seen that the siloxane central core was slightly unstable to other procedures involving oxidation of aldehydes or hydrolysis of methyl esters to recover the acid. The introduction of the additional vinyl group in this reaction step also slightly red shifts the dye color by increasing the conjugation between the acid anchor and dye core.

The absorption spectra of **LBG1** and **LBG3** measured in chloroform are displayed in Figure 2a. Extinction coefficients and absorption maxima are summarized in Table 1. Both **LBG1** and **LBG3** dyes exhibit high molar extinction coefficients that compare favorably to other Pc dyes^{7,9,14} and organic sensitizers.¹⁵ **LBG3** displays a bluish green

color between the blue color of *tert*-butyl-SiPc and the green color of **LBG1** (Figure S12). The spectra of both compounds exhibit a similar absorption peak for the Soret bands at 355 nm. In addition, the molar extinction coefficients of the Soret bands of both dyes are on the order of $10^5 \text{ M}^{-1} \text{ cm}^{-1}$, allowing for efficient photon harvesting in the blue region of the spectrum.¹⁶ The Q-band in **LBG3** exhibited a significant blue shift of the absorption maximum to 705 nm compared to 786 nm for **LBG1**. In comparison with **LBG1**, *tert*-butyl SiPc and *tert*-butyl SiNc, **LBG3** exhibits optical properties between SiPc and SiNc (Figure S13). This design approach to make hybrid dyes between a Pc and an Nc allows for a gradual red shift of the absorption spectrum.

Table 1. Optical and Electrochemical Data for **LBG3** and **LBG1**

dye	λ_{max} [nm]	ϵ_{max} [$\text{M}^{-1} \text{ cm}^{-1}$]	$E_{\text{g, opt}}^a$ [eV]	$E_{\text{ox}}/E_{\text{red}}^b$ [E(V) vs NHE]	$E_{\text{g, EC}}^c$ [eV]
LBG3	705	2.67×10^5	1.68	1.02/−0.57	1.59
LBG1	786	3.11×10^5	1.43	0.80/−0.50	1.30

^a Optical band gap was estimated from UV–vis absorption onset.

^b Assuming the redox potential of the Fc^+/Fc standard to be 0.70 V vs Normal Hydrogen Electrode (NHE). ^c Electrochemical band gap.

The oxidation and reduction potentials of **LBG1** and **LBG3** were measured by cyclic voltammetry (CV) in dichloromethane containing 0.1 M of TBAPF₆ (see Figure S14). The electrochemical data are given in Table 1. The reduction potential, E_{red} , of **LBG3** shows a $\sim 70 \text{ mV}$ cathodic shift compared to **LBG1** due to decreased conjugation. **LBG3** thus has a slightly larger driving force for electron injection into the conduction band of TiO_2 (−0.50 V vs NHE)¹⁶ compared to **LBG1** (Figure 2b). The oxidation potential, E_{ox} , of **LBG3** exhibits a significant anodic shift (220 mV) compared to **LBG1** (Figure 2b), which should result in a more efficient regeneration of dye by the I^-/I_3^- redox shuttle (+0.35 V vs NHE).¹⁷

Typical required driving forces for electron injection from sensitizing dyes into titania are on the order of tenths of an eV.¹⁸ Conversely, the thermodynamic driving force required for the regeneration of oxidized dyes by the I^-/I_3^- redox shuttle has been shown to be at least 0.4 eV.¹⁹ Judging from the measured CV data of **LBG1** and **LBG3**, the energetic offset of the dyes' HOMO/LUMO values are insufficient for efficient DSC operation. However, while the redox potential is held constant at a given I^-/I_3^- concentration due to the Nernst equation, the TiO_2 conduction band can be shifted by dipoles and the addition of ions in the electrolyte. This can drastically affect the

(13) Katayose, M.; Tai, S.; Kamijima, K.; Hagiwara, H.; Hayashi, N. *J. Chem. Soc., Perkin Trans. 2* **1992**, 403.

(14) (a) Cid, J.-J.; Yum, J.-H.; Jang, S.-R.; Nazeeruddin, M. K.; Martinez-Ferrero, E.; Palomares, E.; Ko, J.; Grätzel, M.; Torres, T. *Angew. Chem., Int. Ed.* **2007**, *46*, 8358. (b) Kimura, M.; Nomoto, H.; Masaki, N.; Mori, S. *Angew. Chem., Int. Ed.* **2012**, *51*, 4371.

(15) Gao, P.; Tsao, H. N.; Grätzel, M.; Nazeeruddin, M. K. *Org. Lett.* **2012**, *14*, 4330.

(16) Hsieh, C.-P.; Lu, H.-P.; Chiu, C.-L.; Lee, C.-W.; Chuang, S.-H.; Mai, C.-L.; Yen, W.-N.; Hsu, S.-J.; Diao, E. W.-G.; Yeh, C.-Y. *J. Mater. Chem.* **2010**, *20*, 1127.

(17) Boschloo, G.; Gibson, E. A.; Hagfeldt, A. *J. Phys. Chem. Lett.* **2011**, *2*, 3016.

(18) (a) Cai, J.; Satoh, N.; Han, L. *J. Phys. Chem. C* **2011**, *115*, 6033. (b) Koops, S. E.; O'Regan, B. C.; Barnes, P. R. F.; Durrant, J. R. *J. Am. Chem. Soc.* **2009**, *131*, 4808.

(19) Boschloo, G.; Hagfeldt, A. *Acc. Chem. Res.* **2009**, *42*, 1819.

electron injection efficiency.^{18b,19} The electrolyte additives 4-*tert*-butylpyridine and guanidinium thiocyanate typically increase the efficiency of DSCs by shifting the conduction band negative vs NHE.²⁰ These additives resulted in poor device performance for **LBG1** and **LBG3** and were therefore omitted from the electrolyte. Instead an electrolyte with a higher concentration of Li (1.0 M LiI, 0.05 M I₂) was used in the devices for optimal performance, as lithium ions have been reported to shift the titania conduction band more positive with respect to NHE.²⁰

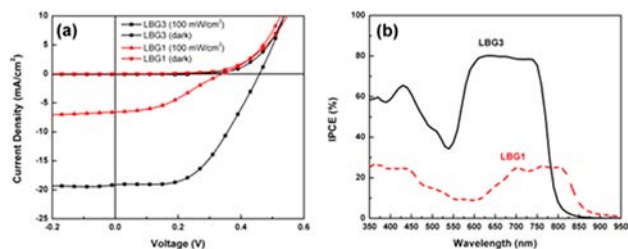


Figure 3. (a) J – V characteristic of DSCs sensitized by **LBG1** and **LBG3** measured under illumination with simulated AM 1.5G sunlight and in the dark and (b) IPCE spectra of DSCs sensitized by **LBG1** and **LBG3**.

LBG1 and **LBG3** sensitized DSCs were fabricated using substrates with 8 μm of standard 20 nm particle titania paste, along with a 5 μm thick scattering layer. Device J – V characteristics are depicted in Figure 3a. **LBG1** achieves a short-circuit photocurrent (J_{sc}) of 6.56 mA/cm², an open circuit voltage (V_{oc}) of 0.36 V, and a fill factor (ff) of 0.38 for a total efficiency of 0.9%. While the low voltage can be attributed to the relatively low level of the titania conduction band, the J – V curve of the **LBG1**-based devices also displays a distinct s-kink, indicative of an energetic barrier. It is suspected that this is due to the offset between the I[–]/I₃[–] redox potential and **LBG1** HOMO being too small for efficient regeneration, and limits the ff of the device.²¹ It should be noted that the relatively large energetic offset needed for efficient dye regeneration is due to the complex regeneration kinetics involving formation of intermediates such as the I₂[–] radical.²² The potential of I₂[–]/I[–] determined by the photomodulated voltammetry is found to be \sim 0.79 V vs. NHE,¹⁷ which is very close to the E_{ox} of **LBG1**. S-Kinks have been previously seen when the dye HOMO is too close to the redox potential for efficient regeneration.²¹ Cells based on **LBG3**, on the other hand, do not display such an s-kink, which can be explained by the 0.62 eV difference between **LBG3**'s E_{ox} and the redox potential of

I[–]/I₃[–]. **LBG3** devices display high photocurrents of 19.0 mA/cm², a V_{oc} of 0.46 V, and an ff of 0.51 for a total efficiency of 4.5%. The high photocurrent of these cells reflects the large amount of absorbed photons in the near-IR region of the solar spectrum and **LBG3**'s efficient photoresponse in this region. Despite the low V_{oc} , **LBG3** achieves very high photocurrents and relatively good efficiencies for such a red-absorbing sensitizer.

The incident photon to current conversion efficiency (IPCE) of **LBG1** and **LBG3** devices is displayed in Figure 3b. The **LBG1** device exhibits a broad IPCE between 650 and 850 nm, but its peak IPCE is limited to approximately 25–30%. On the other hand, **LBG3** shows a broad flat IPCE of 80% between 600 and 750 nm. The strong photoresponse in the red and near-infrared make **LBG3** an excellent candidate for use as a low band gap solar cell in current matched DSC tandems. The intense green color and relative transparency in the green portion of the spectrum may also make this dye an interesting compound for efficient semitransparent building integrated photovoltaics.

To summarize, we have used synthetic approaches to combine naphthalo- and phthalocyanine moieties into a novel, efficient red-absorbing sensitizing dye, **LBG3**. The absorption of **LBG3** is red-shifted compared to typical phthalocyanine sensitizers while maintaining the energy levels necessary for efficient electron injection and hole regeneration. In addition, the central Si-atom of **LBG3** allows for the attachment of bulky alkyl side chains for additional functionality such as minimizing recombination, increasing solubility, and mitigating dye aggregation. **LBG3**-based DSCs achieve very high photocurrents making it an attractive sensitizer for applications such as cosensitization, energy relay dye devices, and DSC tandem solar cells. The hybrid molecular engineering approach demonstrated herein is an example of the possibility to prepare new types of chromophores by merging elements of phthalocyanines, porphyrins, naphthalocyanines, and other dyes. This is a method to fine-tune the band gap and energetics of DSC sensitizer dyes to further boost record efficiencies.

Acknowledgment. This work was supported by the Office of Naval Research (ONR) through Grant N000141110244. B.L. thanks Theresa McLaughlin of the Stanford University Mass Spectrometry Group for HRMS analysis. E.L.U. thanks the Marcus and Amalia Wallenberg memorial fund for financial support.

Supporting Information Available. General experimental procedures, DSCs fabrication and analytical data reported herein. This material is available free of charge via the Internet at <http://pubs.acs.org>.

The authors declare no competing financial interest.

(20) Raga, S. R.; Barea, E. M.; Fabregat-Santiago, F. *J. Phys. Chem. Lett.* **2012**, 1629.

(21) Liu, Y.; Jennings, J. R.; Parameswaran, M.; Wang, Q. *Energy Environ. Sci.* **2011**, 4, 564.

(22) Pelet, S.; Moser, J.-E.; Grätzel, M. *J. Phys. Chem. B* **2000**, 104, 1791.